Exon Utilization Improves Risk Stratification for Advanced Heart Failure in Titin Cardiomyopathy

Peter Deckerman[1], Jihyeon Lee[1], Aleksandra Binek[1], Sarah Parker[1], Daniel J. Luthringer[1], Michelle M. Kittleson[1], Donald Richards[1], Ian Williamson[1], Daria Ma[1], Lawrence S.C. Czer[1], Nan Jiang[1], Jason Cowan[2], Ray E. Hershberger[2], Jennifer E. Van Eyk[1], Evan P. Kransdorf[1]

1-Smidt Heart Institute, Cedars-Sinai Medical Center, Los Angeles, CA 90048, USA

2-Davis Heart and Lung Research Institute, The Ohio State University, Columbus, OH 43210, USA

Correspondence:

Evan Kransdorf, MD, PhD

8670 Wilshire Blvd., Suite 200

Beverly Hills, CA 90211

Evan.kransdorf@cshs.org

(310) 248-300

Word Count: 7368

Abstract

Truncating variants in the titin (TTN) gene (TTN-TV) are the most common genetic cause of dilated cardiomyopathy (DCM) and confer a significant risk of progression to advanced heart failure (AHF). Penetrance of TTN-TV has been linked to the level of expression of the exon containing the TTN-TV, quantified using the percent spliced in (PSI). We performed long-read RNA sequencing on cardiac tissue from 8 unused organ donors and 14 DCM patients and identified expression of 16 *TTN* isoforms. We used these data to recalculate PSI (PSI-LR). PSI-LR reclassified 5% of exons compared to the original PSI calculated using short-read RNA sequencing (PSI-SR). We then analyzed a cohort of 98 patients with cardiomyopathy due to TTN-TV, 34 (35%) of whom developed AHF, as defined as the need for left ventricular assist device implantation or heart transplant. PSI-LR, but not the original PSI-SR, predicted AHF risk (odds ratio 1.35 per 0.1 increase, p=0.038). A PSI-LR threshold of <0.75 best identified patients who did not progress to AHF. Our PSI metric, PSI-LR, which accounts for the expression of the multiple *TTN* isoforms, predicts the expressivity of TTN-TV with regards to the progression to AHF, which has important implications for prognosis and management.

Introduction

Rare DNA variants which lead to truncation of transcript translation via stop codon gain, frameshift, or a splice donor/acceptor mutation in the gene titin (*TTN*) are the most common genetic cause of dilated cardiomyopathy (DCM), identified in 10%-20% of patients (1). DCM due to *TTN* truncating variants (TTN-TV) is among the most responsive to heart failure medical therapy, with left ventricular (LV) reverse remodeling observed in 50-60% of cases (2-4). However, a paradox exists because TTN-TVs are also the most frequently identified genetic cause of end-stage heart failure that requires heart transplantation (HT) (5).

The meta-transcript of the *TTN* gene has 363 coding exons which in turn encode a 35,991 amino acid protein that connects the M-line to Z-line of the sarcomere (6) and contributes to the passive tension of the cardiomyocyte (7). TTN is transcribed into several isoforms, with the predominantly expressed isoforms in adult cardiomyocytes being N2BA and N2B (7, 8). However, the shorter isoforms, Novex-3 (9) and Cronos (10), also have important functions in both fetal and adult cardiomyocytes.

TTN-TVs can be identified in up to 1-3% of the population (8, 11). However, prior studies have shown that patients with DCM carry a preponderance of TTN-TVs in the A-band (8, 12). The expression levels of transcribed *TTN* exons within 3 main isoforms (*TTN* N2BA, N2B, Novex-3) have been used to calculate the percent spliced in (PSI), which quantitates the fraction of transcripts that include a particular exon, and patients with TTN-TVs affecting exons with a PSI > 0.9 (included in >90% of transcripts) were more likely to develop DCM (8). As a result, the American College of Medical Genetics and Genomics (ACMG) criteria for variant interpretation in DCM, which originally required a causative TTN-TV to originate in the A-band (13), were

revised to include variants affecting high PSI exons (PSI > 0.9) outside the A-band (1). There is an association between DCM and TTN-TVs in high PSI exons within the Z-disk, I-band, A-band, and M-band, but interestingly, also TTN-TV in a limited number of low PSI (0.15 to 0.48) I-band exons (14). Furthermore, there are numerous A-band exons with PSI > 0.9 that do not exhibit significant enrichment in DCM. These findings suggest that A-band restrictive views of genetic DCM may be both scientifically and clinically limiting.

The development of DCM in patients carrying TTN-TV, *i.e.* penetrance, differs from the severity of DCM that develops, *i.e.* expressivity (15, 16). The ability to predict which patients with DCM due to TTN-TV will have high expressivity and develop advanced heart failure (AHF) requiring specialized therapies including durable left ventricular assist device (LVAD) implantation or HT represents a critical but unmet clinical need. Given the important contribution of exon utilization to the penetrance of TTN-TV, as quantified using PSI, we hypothesized that PSI considering all *TTN* isoforms (beyond N2BA, N2B, and Novex-3) would predict the risk of AHF in patients with DCM due to TTN-TV. We sought to recalculate PSI considering all *TTN* isoforms and investigate the utility of this novel PSI to predict AHF.

Methods

Sex As a Biological Variable

Our study included both men and women.

Cardiac Tissue for RNA, Spatial Transcriptomics, and Proteomic Studies

This study was performed under protocols approved by the Cedars-Sinai Institutional Review Board (Pro00010979, STUDY00001617, STUDY00004096) and OneLegacy. All tissue donors provided consent to participate. We utilized a total of 40 samples from 33 heart explants: 22 samples for long-read RNA sequencing, 4 for spatial transcriptomics, and 14 for proteomics. Samples for long-read RNA sequencing were derived from donors from 2 groups: 8 organ donors not utilized for HT (group 1) and 14 patients undergoing HT for end-stage DCM (group 2). For spatial transcriptomics, samples were derived from 1 organ donor not utilized for HT and 3 patients undergoing HT for end-stage DCM (group 3). For proteomics, samples were derived from 14 patients undergoing HT for end-stage DCM (group 4). Characteristics and genetic testing results for all tissue donors is provided in Supplemental Tables 1 and 2, respectively.

TTN CM Patient Group

We identified 98 patients from 90 families that presented to the Advanced Heart Disease or Cardiogenetics clinics at Cedars-Sinai Medical Center between 2015 and 2025 for cardiomyopathy due to a TTN-TV (CM-TTN-TV). In addition, we identified patients through search of the Cedars-Sinai electronic medical record via Deep6 AI (17). We defined CM-TTN-TV as left ventricular (LV) ejection fraction < 50% by echocardiography, with or without LV dilation. LV dilation was defined as LV diastolic diameter ≥ 95th percentile for sex/height (18, 19). We defined DCM as the presence of both left ventricular ejection fraction < 50% and left ventricular dilation as defined above (18). Genetic testing results for CM-TTN-TV group is provided in Supplemental Table 3. AHF was defined as the need for LVAD implantation or HT. LV reverse remodeling was defined, in patients who did not have AHF, as improvement of ejection fraction

from first to last available echocardiogram of ≥ 10% or achievement of an ejection fraction of ≥ 40% or more, in patients with an initial EF < 40% (20).

Genetic Testing

Genetic testing was performed using commercial vendors or via whole exome sequencing as part of a biobank study as previously described (21). All genes classified by ClinGen as having a definitive, strong, or moderate association for DCM were tested (Supplemental Table 4) (22). Variant consequence and genomic position were determined using Ensembl Variant Effect Predictor (23) based on the *TTN* meta-transcript (ENST00000589042.5).

RNA Sequencing and Bioinformatics

RNA was isolated from explanted cardiac tissue using Zymo RNA extraction kit (Zymo Research). RNA purification was performed using column purification (Qiagen). Library preparation was performed using the Kinnex full-length RNA kit (PacBio). Parameters of RNA libraries is detailed in Supplementary Table 5. RNA sequencing was performed using SMRT cell on a Revio system (Novogene). The resulting BAM files were mapped to the Gencode version 48 transcriptome (24) modified to include the *TTN* isoform Cronos which originates at a transcriptional start site in the intron between exon 239 and 240 of the *TTN* meta-transcript (10). RNA transcripts for all *TTN* isoforms were quantified using Oarfish (25, 26). Raw counts were converted to transcripts per million (TPM) in a sample-wise fashion (27).

Spatial Transcriptomics

Formalin-fixed paraffin-embedded slides from 4 heart explants were obtained: 1 from an organ donor not utilized for HT, 1 from a patient undergoing HT for end-stage DCM due to a *DSP* variant, and 2 patients undergoing HT for end-stage DCM due to a TTN-TV. The Xenium Human Immuno-Oncology Profiling Panel was utilized with the addition of custom probes for the *TTN* isoforms N2BA, Novex-3, and meta-transcript (designed to span a unique exon-exon junction), *DSP*, and the housekeeping gene glyceraldehyde 3-phosphate dehydrogenase (*GAPDH*). Custom probe sequences are provided in Supplemental Table 6. Probe hybridization, ligation, and rolling circle amplification were performed, following the manufacturer's protocol. Imaging and signal decoding were done using the Xenium Analyzer instrument (10x Genomics). Each slide's Xenium output was exported as a "spatialexperiment" object and normalized using SpaNorm (28). Normalized counts for each slide were rescaled to between 0 and 1000 and plotted using the R package Voyager (29).

Calculation of PSI

We tabulated exon-exon junctions for all *TTN* isoforms in Gencode version 48, except excluding ENST000000470257.1, a non-coding transcript, and including Cronos (Supplemental Table 7). Junction sequences were counted in a sample-wise fashion using Bioconductor (30) Biostrings (31) and converted to TPM. PSI was calculated for *TTN* meta-transcript exons 2 to 362 per the original definition (32):

$$PSI_{exonN} = \frac{\sum IR_{exonN}}{\sum (IR_{exonN} + ER_{exonN})}$$

$$IR = \sum (TPM_{exonN-1} + TPM_{exonN} + TPM_{exonN+1})$$

$$ER = \sum (TPM_{exonN-1} + TPM_{exonN+1})$$

where N=exon number, IR=inclusion reads, ER=exclusion reads. We did not calculate PSI for exons 1 and 363 as exon 1 is non-coding and variants in exon 363 would not be expected to induce nonsense-mediated decay. Furthermore, exon 363 has previously not been associated with DCM (14). The median PSI value for each exon among all samples was utilized and termed PSI-long read (PSI-LR).

Mass Spectrometry-based Proteomics

14 samples underwent proteomics sample processing as previously reported (33). Briefly, protein was isolated from explanted cardiac tissue by the "in sequence" method (add reference) *i.e.*: each tissue was fractionated into cytosolic-, myofilament-, and insoluble-enriched protein fractions, and trypsin digested on S-Trap columns (ProtiFi). Peptides from each patient sample were analyzed in 3 runs by liquid chromatography-tandem mass spectrometry (LC-MS/MS) in data independent acquisition mode on an Ultimate 3000 NanoLC connected to an Orbitrap Fusion™ Lumos™ Tribrid™ Mass Spectrometer (Thermo Fisher Scientific) equipped with an EasySpray ion source. Data acquisition was completed blinded to experimental groups. LC-MS/MS method was adapted and modified from previously published workflow (34). Peptides were separated on a C18 column (15 cm with 300 µm ID, 3 µm Omega Polar C18

beads, and 100 Å pore size, Phenomenex) over the course of total 90 minutes at a flow rate of 8µL/min. Mobile phase A was 0.1% v/v formic acid in water and mobile phase B was 90% ACN, 0.1% formic acid in water. Initial loading condition was 1% B for 3 min and then 3% for another 2 min at a flow rate of 8 µL/min to allow for equilibration and for samples to reach the column, followed by a linear gradient of 3–30% B over 70 min, 30–40% B over 10 min and 40–45& B over 5 min. Each MS1 scan was followed by 150 data independent acquisition (DIA) MS2 scans (35) (4Da size precursor window). Peptide identification and quantification was performed using DIA-NN (36). Spectral library was generated using DIA-NN v1.8.1 by searching two FASTA files: the reviewed human proteome (UniProt, downloaded August 2024) and *TTN* isoform sequences derived from the translation of all 15 *TTN* transcript isoforms. Default settings were used, except that "Generate spectral library" was enabled, "Protein names (from FASTA)" was selected for protein inference, and "Smart profiling" was applied for library generation. In the 14 proteomics samples, peptides mapped to *TTN* isoforms were annotated to their corresponding exons according to the *TTN* meta-transcript translation. Quantification was performed as:

$$Q_{exon} = log \sum (PI_{exon})$$

where Q=quantification for each exon, PI= intensity of peptide mapping to that exon. The intensity of peptides that split across an exon-exon junction were assigned to both exons. Identified peptides are listed in Supplemental Data Set 1.

Statistical Analysis

Univariate logistic modeling with AHF as the response variable was performed using a Gaussian generalized linear model. Cox proportional hazard modeling was performed with the R package "survival" (37). Figures were made using "ggplot2" (38). Matthews correlation coefficient was utilized for assessment of binary classification performance given its superiority over other metrics (39). All analysis was performed using R (40).

Results

TTN Transcript Isoform Quantification

We quantified *TTN* transcript isoforms using heart tissue collected from 22 donors: 8 organ donors not utilized for HT, 7 patients with end-stage DCM without a TTN-TV undergoing HT, and 7 patients with end-stage DCM with a TTN-TV undergoing HT. Among the 7 patients with end-stage DCM without a TTN-TV who underwent HT, 4 had disease-causing variants in other genes associated with DCM including *DMD*, *FLNC*, *LMNA*, and *RBM20* (Supplemental Table 2). In the 7 patients with TTN-TV, variants were all located in *TTN* exons with PSI of 1.0 (Supplemental Table 2).

To assess *TTN* transcript isoform expression levels, we quantified long-read sequencing-derived RNA expression levels of all 15 *TTN* transcript isoforms curated in Gencode, as well as Cronos, which was manually curated, with long-read RNA sequencing. The top 5 most highly expressed isoforms across the three groups were N2BA, Novex-3, N2B, TTN-208, and TTN-211 (Table 1). Notably, the *TTN* meta-transcript, which is the default *TTN* transcript as defined by the Matched Annotation from NCBI and EMBL-EBI (MANE) project, was in the bottom half of

TTN transcript isoforms by expression levels. Given that this transcript is used for variant interpretation, it is notable that it is transcribed at low levels. Cronos was the transcript with the lowest expression.

We then compared *TTN* transcript isoform expression levels among the 3 groups of cardiac tissue samples (Table 1). We found that the expression of 6 isoforms differed among the groups: N2BA, Novex-3, TTN-208, TTN-211, TTN-215, and N2A. Comparing samples from organ donors to all patients with DCM (Supplemental Table 8), expression levels of the above 6 isoforms were significantly different, as were the meta-transcript and Novex-2. Isoform expression was lower in samples from patients with DCM for all isoforms except the meta-transcript. Comparing samples from patients with DCM not due to a TTN-TV to those with DCM due to a TTN-TV, isoform expression was similar except for TTN-211, which was more highly expressed in DCM due to a TTN-TV (Supplemental Table 9). Although not significant, there was also a trend towards higher Novex-3 and TTN-208 expression in DCM due to a TTN-TV (Supplemental Table 9). Taken together, these results show: (1) multiple *TTN* transcript isoforms are expressed in humans, (2) isoform expression is generally lower in DCM as compared to normal tissue, and (3) there may be a compensatory increase in a limited number of isoforms in DCM due to a TTN-TV, as was seen for TTN-211.

Spatial Transcriptomics

We sought to use spatial transcriptomics to validate the isoform expression levels we measured using long-read RNA sequencing. We performed spatial transcriptomics using the Xenium platform on heart tissue collected from 4 donors: 1 organ donor, 1 patient that

underwent HT for DCM due to a *DSP* disease-causing variant, and 2 patients that underwent HT for DCM due to TTN-TV. We developed isoform-specific probes for highly expressed *TTN* isoforms with unique spice junctions: N2BA, Novex-3, and meta-transcript. For all 4 donors, we found that the count ratio of *TTN* Novex-3 to N2BA and meta-transcript to N2BA were similar between those derived from long-read RNA sequencing and spatial transcriptomics (Figure 1A to 1D and Supplemental Table 10). These results validate the accuracy of our *TTN* isoform quantification obtained by long-read RNA sequencing.

Calculation of PSI

To determine any differences in exon-specific PSI between our cohort and previously reported benchmarks from Roberts et al. (8), we quantified exon-exon junction expression for all junctions present in *TTN* transcript isoforms in Gencode using long-read RNA sequencing, calculated exon-specific PSI (based on exons in the *TTN* meta-transcript) for each sample, and found the median value across the DCM samples (Supplemental Table 11 and Figure 2A). We have termed this metric PSI-LR. We compared the PSI-LR values to those calculated by Roberts *et. al*. using short-read RNA sequencing (PSI-SR) and found that PSI-LR was higher than PSI-SR for 84 exons, 77/84 (92%) of which were I-band, 6/84 in the Z-disk, 1/84 in the M-band, and 0/84 in the A-band. PSI-LR was also lower than PSI-SR for 239 exons, 129/239 (54%) in the I-band, 106/239 (44%) in the A-band, 4/239 in the M-band, and 0/239 in the Z-disk (Figure 2B). The overall correlation between PSI-LR and PSI-SR was 0.92.

Roberts *et. al.* classified *TTN* exons with a PSI of <0.15 as low, 0.15-0.9 as intermediate, and >0.9 as high usage (8). We assessed the reclassification of exons using PSI-LR as compared

to PSI-SR and found that 299/361 exons (82%) did not change usage classification, whereas 62 exons did change usage classification. More specifically, 10/361 exons (3%) increased to high usage, 9/361 exons (2%) decreased from high usage, and 43/361 (12%) changed within the low/intermediate usage classes (Figure 2C).

Taken together, these results show that our novel PSI values result in reclassification of 3% of exons to and 2% of exons from the high usage group.

Mass spectrometry-based TTN Peptide Mapping

To analyze TTN isoform expression at the protein level, we performed mass spectrometry-based proteomics on explanted cardiac tissue from 14 patients undergoing HT: 10 for DCM not due to a TTN-TV and 4 for DCM not due to a TTN-TV. We observed 2490 unique TTN prototypic peptides represented by 3580 total precursors comprised of redundant TTN peptides with various charge states and/or post-translational modifications (Supplemental Data Set 1). First, we sought to identify which *TTN* isoforms were represented by the 2490 unique TTN peptides. Of the 16 *TTN* transcript isoforms, 15 yield proteins (Supplemental Table 7), as TTN-211 does not contain an open reading frame. Of these 15 isoforms, 9 isoforms generate peptides that are unique to one specific isoform. Overall, the majority (96%, 2397/2490 peptides) of the *TTN* peptides were not unique and mapped to one or more of 6 isoforms, 4% (93/2490 peptides) were specific to a single unique isoform: 92 mapped uniquely to Novex-3, and 1 peptide mapped uniquely to TTN-215 (Supplemental Data Set 1).

Next, we determined the peptide abundance from *TTN* meta-transcript exons 2 to 362 (Figure 3) based on the 3580 *TTN* peptides. Of these, 3424 were present in the meta-transcript

and mapped to a single site within the protein. There were 1/27 exons in the Z-disk (4%), 105/223 exons in the I-band (47%), 1/106 exons in the A-band (1%), and 0/5 exons in the M-band for which we did not identify any peptides. Excluding exons without any identified peptides, the median log peptide abundance for the Z-disk, I-band, A-band and M-band were 16.0, 14.6, 16.5, and 15.5, respectively.

We next sought to determine the ability of PSI-LR and PSI-SR to predict *TTN* peptide abundance. Both PSI-LR and PSI-SR predicted the detection of ≥ 1 peptide from a *TTN* exon, with an area under the precision-recall curve (AUPRC) of 0.94 and 0.89, respectively. For PSI-LR, 39/102 exons (38%) were predicted to be low (PSI-LR < 0.15) usage yielded peptides, whereas 11/189 exons (6%) were predicted to be high (PSI-LR > 0.90) usage yielded no peptides. In contrast, 20/103 exons (19%) were predicted to be low (PSI-SR < 0.15) usage yielded peptides, whereas 8/186 exons (4%) were predicted to be high (PSI-SR > 0.90) usage yielded no peptides.

Given that haploinsufficiency has been reported to be an important mechanism of pathogenesis in DCM due to a TTN-TV (41), we sought to determine if there was a lower total *TTN* peptide abundance in the 4 patients with DCM due to a TTN-TV as compared to the 10 patients with DCM not attributed to TTN-TV. Interestingly, the total *TTN* peptide abundance did not differ between the two groups (p=0.831). We then sought to determine if there was a lower exon-specific *TTN* peptide abundance in the 4 patients with DCM due to a TTN-TV as compared to the 10 patients with DCM not attributed to TTN-TV. For the 267/362 exons with associated peptides, there was no difference in peptide abundance between the groups for 254/267 exons, but surprisingly there was significantly higher peptide abundance in patients with DCM due to a TTN-TV specifically for 13/267 exons (Supplemental Table 12). Interestingly, all 13 of

these exons are present in *TTN* isoform TTN-208 which was expressed at higher levels in patients with DCM due to a TTN-TV (Supplemental Table 9, p=0.085), 9 are present in Novex-3 which was expressed at higher levels in patients with DCM due to a TTN-TV (Supplemental Table 9, p=0.064), and 2 are present in TTN-211 which was expressed at higher levels in patients with DCM due to a TTN-TV (Supplemental Table 9, p=0.002).

Taken together, these protein-level data suggest several findings: (1) the non-canonical *TTN* isoforms Novex-3 and TTN-215 are present *in vivo* in patients with DCM with AHF, (2) there is disassociation between exon-level PSI and the level of peptides derived from individual exons such that peptides from some low usage exons are detectable, and (3) DCM due to a TTN-TV may be associated with an increase in expression of certain *TTN* isoforms, rather than a deficiency.

Predictors of Advanced Heart Failure in TTN Cardiomyopathy

The next step was to perform clinical validation of the PSI-LR in individuals with cardiomyopathy due to TTN-TV (CM-TTN-TV). We identified 98 patients that were seen at Cedars-Sinai between 2015 and 2025 with cardiomyopathy and a likely pathogenic or pathogenic variant (LP/P) in the *TTN* gene. No patients possessed LP/P variants in any other DCM-associated genes. All patients were treated with guideline-directed medical therapy. During the study period 34 (35%) patients developed AHF, as defined by the need for implantation of LVAD or HT. Characteristics of patients with AHF are provided in Table 2. Patients with AHF were more frequently male (85% vs. 66%, p=0.066), more frequently had a history of hypertension (56% vs 30%, p=0.031), but displayed a lower systolic blood pressure at

their first visit (106 mmHg vs. 116 mmHg, p=0.005), and more frequently had a history of ventricular tachycardia (76% vs. 33%, p<0.001). Patients with AHF had a lower ejection fraction at their first (20% vs. 28%, p=0.016) and final visits (16% vs. 44%, p<0.001) and were less likely to achieve left ventricular reverse remodeling over time (3% vs. 52%, p<0.001).

Genetic characteristics of patients with CM-TTN-TV that developed AHF are provided in Table 3. Patients with AHF more frequently had variants in exons comprising the A-band (88% vs. 71%, p=0.159) and these exons were more frequently classified as high usage exons by both PSI-LR (62% vs. 47%, p=0.071) or PSI-SR (100% vs. 84%, p=0.042). In the 34 patients with AHF, PSI-LR values were lower (Figure 4A, median 0.98, range 0.76-1.00) than PSI-SR values (all values were 1.0, p<0.001). A PSI-LR value of 0.75 yielded the highest Matthews correlation coefficient (MCC) (Supplemental Figure 1), whereas there was no optimal point for PSI-SR (Supplemental Figure 2).

In univariate analysis, we identified four variables associated with the risk of AHF (Table 4): female sex (OR 0.33, 95% confidence interval [CI] 0.11-0.97, p=0.044), black race (OR 4.90, 95% CI 1.33-18.1, p=0.017), history of hypertension (OR 2.79, 95% CI 1.18-6.58, p=0.019), and exon utilization as measured using PSI-LR (OR 1.35 per 0.1 increase, 95% CI 1.02-1.79, p=0.038). We found that exon utilization as measured using PSI-SR was not associated with an increased risk of AHF. Model coefficients were uninterpretable due to multicollinearity, as all patients with AHF had PSI-SR values of 1. Interestingly, TTN peptide abundance did not predict AHF (OR 1.03, 95% CI 0.91-1.16, p=0.680)

We sought to determine if exon utilization predicted the age at which an AHF-intervention, either LVAD implantation or HT occurred. Using a Cox proportional hazards

model, we found that exon utilization as measured using PSI-LR was associated with age of AHF intervention (HR 2.05 per 0.1 increase, 95% CI 1.03-7.80, p=0.047) whereas exon utilization as measured using PSI-SR was not associated, again with uninterpretable coefficients due to multicollinearity. No patients with CM-TTN-TV and a PSI-LR of less than 0.75 developed AHF, whereas survival free of AHF was 0.28 (95% CI 0.15-0.53) by age 73 in patients with PSI-LR ≥ 0.75 (Figure 4B).

Discussion

In this study, we investigated *TTN* transcript isoform levels using long-read RNA sequencing in explanted cardiac tissue from organ donors and patients with end-stage DCM undergoing HT. We found that multiple *TTN* transcript isoforms are expressed in humans, isoform expression is generally lower in DCM as compared to normal tissue, and that there may be a compensatory increase in a limited number of isoforms in DCM due to a TTN-TV. We validated our *TTN* transcript isoform level measurements using spatial transcriptomics. We recalculated exon-specific PSI values in consideration of the multiple *TTN* transcript isoforms and our novel PSI values resulted in reclassification of 3% of exons to the high usage group (PSI > 0.9) and 2% of exons from the high usage group. We also performed mass spectrometry proteomics and found that the non-canonical *TTN* isoforms Novex-3 and TTN-215 proteins are present *in vivo*. We found a disassociation between exon-level PSI and the abundance of peptides derived from individual exons such that peptides from some low usage exons are detectable, and that DCM due to a TTN-TV may be associated with an increase in RNA-level expression of certain *TTN* isoforms. This protein isoform level data is consistent with our

observations based on *TTN* transcript isoform expression. Finally, we sought to determine if exon utilization predicted the development of AHF as well as the age at which AHF intervention occurred. Using both Cox proportional hazards and logistic modeling, we found that our novel PSI-LR values predicted the risk of AHF, whereas the PSI-SR did not. Thus, PSI-LR represents an important new marker of TTN-TV expressivity.

These results have several important clinical implications. First, the clinical significance of TTN-TV that occur in the I-band of TTN has been debated, as these variants are less common in patients with end-stage heart failure as compared to variants in the A-band (8) and PSI values of 102/223 exons (46%) of the I-band are in the low usage range (PSI-LR < 0.15). However, our results show that I-band variants are associated with CM. Given that we detected TTN derived peptides from 39/102 exons (38%) with low usage, a low PSI should not be used as the sole criteria to discount the clinical significance of a TTN-TV, supported by prior observations (14). Furthermore, our findings show that if the PSI-LR of the exon containing the TTN-TV is < 0.75, CM did not progress to AHF. In patients with TTN-TV in exons with a PSI-LR ≥ 0.75, however, there is a substantially increased risk of progression to AHF. Thus, patients with PSI-LR < 0.75 should be targeted for maximal guideline directed medical therapy (GDMT) with a goal of LV reverse remodeling and recovery, whereas patients with PSI-LR ≥ 0.75 should be followed closely and considered for earlier referral for consideration of AHF therapies such as LVAD and HT.

A significant portion of patients diagnosed with DCM will have some degree of LV reverse remodeling, whereas a smaller portion of patients will progress to end-stage heart disease (4, 42). Consistent with these observations, in the group of CM-TTN-TV patients

described here, 35% progressed to AHF, but among those that did not develop AHF, the majority of patients (52%) exhibited LV reverse remodeling. All patients in our CM-TTN-TV group were treated with GDMT. Although it is well described that GDMT abrogates important neurohormonal pathways such as the beta-adrenergic (43) and renin-angiotensin-aldosterone systems (44), the specific effects of these agents on *TTN* isoform expression have not been described. We observed that patients undergoing HT for DCM due to a TTN-TV had significantly higher expression of *TTN* transcript isoform TTN-211 and a trend towards higher expression of *TTN* transcript isoforms Novex-3 and TTN-208, changes that were mirrored by elevation of peptides that comprise these isoforms. These findings suggest that there may be compensatory changes in TTN isoforms, potentially in response to GDMT, that occurs in CM-TTN-TV. Further investigation is needed to confirm and elucidate these findings.

Our results also have important implications for the mechanism of DCM due to a TTN-TV. First, the *TTN* isoform Cronos was previously proposed to have important role in DCM (10, 45). However, given our observation of very low levels of Cronos *in vivo*, the role for this isoform is likely more important in cardiomyocyte development than in the adult or diseased state (46). Next, haploinsufficiency has been previously reported to be an important mechanism of pathogenesis in DCM due to a TTN-TV (41). However, we failed to identify decreased TTN peptide levels in 4 patients with DCM due to a TTN-TV, and in fact, we identified higher peptide abundance for a limited number of TTN exons. These results are congruent with those of groups that have found that truncated TTN proteins are integrated into the sarcomere (47, 48) and have a dominant negative effect (8). This, in turn, has implications for future

genetic therapies for TTN-CM, as gene replacement may not be effective, whereas gene editing may be curative.

This study has several strengths and weaknesses. A substantial number of studies of *TTN* expression have relied on animal models. A strength of this work is that these observations offer direct clinical translation by having examined explanted heart tissue from human organ donors and patients undergoing HT for DCM with and without TTN-TV. However, as only a small number of samples were analyzed, the PSI values should not be considered definitive, and additional studies using a comprehensive set of samples representative of patients with DCM are needed. While this study is among the first to utilize long-read RNA sequencing to analyze *TTN* isoforms and expression, only the role of transcript isoforms identified in HAVANA was assessed. Given the large size of *TTN*, other novel transcripts and protein isoforms may be relevant for DCM. Our group of patients with CM-TTN-TV was derived from one AHF program and as such our results need to be validated in a group of patients with a broader severity of CM-TTN-TV and should specifically be validated with respect to penetrance as measured by specific clinical metrics as we have done in this study rather than only by expressivity.

In conclusion, DCM due to a TTN-TV remains the most common cause of DCM, and therefore, the findings here have important translational and clinical implications for the care of patients with DCM. Further validation of the novel metric, PSI-LR, in additional DCM cohorts is needed. Additionally, the high levels of expression of multiple *TTN* isoforms with an unknown physiologic role warrant further investigation to establish the role of these isoforms in health and disease.

Acknowledgements/Funding

This work was funded by seed money support from the Smidt Discovery Fund of the Smidt Heart Institute (E.K.), the American Heart Association (AHA) Postdoctoral Fellowship, AHA Award Number: 829444 (A.B.) and National Institutes of Health (NIH) 1R01HL155346-01A1 (J.V.E.) and 1R01HL144509-01 (J.V.E.). J.V.E. is the Erika Glazer Endowed Chair in Women's Heart Health. We would also like to acknowledge access to mass spectrometers via the Cedars-Sinai Medical Center Proteomics and Metabolomics Core.

References

1. Jordan E, Kinnamon DD, Haas GJ, Hofmeyer M, Kransdorf E, Ewald GA, et al. Genetic Architecture of Dilated Cardiomyopathy in Individuals of African and European Ancestry. *JAMA.* 2023;330(5):432–41.
2. Jansweijer JA, Nieuwhof K, Russo F, Hoorntje ET, Jongbloed JD, Lekanne Deprez RH, et al. Truncating titin mutations are associated with a mild and treatable form of dilated cardiomyopathy. *Eur J Heart Fail.* 2017;19(4):512–21.
3. Verdonschot JAJ, Hazebroek MR, Wang P, Sanders-van Wijk S, Merken JJ, Adriaansen YA, et al. Clinical Phenotype and Genotype Associations With Improvement in Left Ventricular Function in Dilated Cardiomyopathy. *Circ Heart Fail.* 2018;11(11):e005220.
4. Escobar-Lopez L, Ochoa JP, Mirelis JG, Espinosa MA, Navarro M, Gallego-Delgado M, et al. Association of Genetic Variants With Outcomes in Patients With Nonischemic Dilated Cardiomyopathy. *J Am Coll Cardiol.* 2021;78(17):1682–99.

5. Kim Y, Gunnarsdottir OB, Viveiros A, Reichart D, Quiat D, Willcox JAL, et al. Genetic Contribution to End-Stage Cardiomyopathy Requiring Heart Transplantation. *Circ Genom Precis Med.* 2023;16(5):452–61.

6. Furst DO, Osborn M, Nave R, and Weber K. The organization of titin filaments in the half-sarcomere revealed by monoclonal antibodies in immunoelectron microscopy: a map of ten nonrepetitive epitopes starting at the Z line extends close to the M line. *J Cell Biol.* 1988;106(5):1563–72.

7. van der Pijl R, Nusayr E, Strom J, Slater R, Gohlke J, Hourani Z, et al. Importance of N2BA Titin in Maintaining Cardiac Homeostasis and Its Role in Dilated Cardiomyopathy. *Circ Heart Fail.* 2025;18(3):e012083.

8. Roberts AM, Ware JS, Herman DS, Schafer S, Baksi J, Bick AG, et al. Integrated allelic, transcriptional, and phenomic dissection of the cardiac effects of titin truncations in health and disease. *Sci Transl Med.* 2015;7(270):270ra6.

9. Hashimoto K, Ohira M, Kodama A, Kimoto M, Inoue M, Tone S, et al. Loss of connectin novex-3 leads to heart dysfunction associated with impaired cardiomyocyte proliferation and abnormal nuclear mechanics. *Sci Rep.* 2024;14(1):13727.

10. Zou J, Tran D, Baalbaki M, Tang LF, Poon A, Pelonero A, et al. An internal promoter underlies the difference in disease severity between N- and C-terminal truncation mutations of Titin in zebrafish. *Elife.* 2015;4:e09406.

11. Golbus JR, Puckelwartz MJ, Fahrenbach JP, Dellefave-Castillo LM, Wolfgeher D, and McNally EM. Population-based variation in cardiomyopathy genes. *Circ Cardiovasc Genet.* 2012;5(4):391–9.

12. Herman DS, Lam L, Taylor MR, Wang L, Teekakirikul P, Christodoulou D, et al. Truncations of titin causing dilated cardiomyopathy. *N Engl J Med.* 2012;366(7):619–28.

13. Morales A, Kinnamon DD, Jordan E, Platt J, Vatta M, Dorschner MO, et al. Variant Interpretation for Dilated Cardiomyopathy: Refinement of the American College of Medical Genetics and Genomics/ClinGen Guidelines for the DCM Precision Medicine Study. *Circ Genom Precis Med.* 2020;13(2):e002480.

14. Vatta M, Regalado E, Parfenov M, Swartzlander D, Nagl A, Mannello M, et al. Analysis of TTN Truncating Variants in >74 000 Cases Reveals New Clinically Relevant Gene Regions. *Circ Genom Precis Med.* 2025;18(2):e004982.

15. Shah RA, Asatryan B, Sharaf Dabbagh G, Aung N, Khanji MY, Lopes LR, et al. Frequency, Penetrance, and Variable Expressivity of Dilated Cardiomyopathy-Associated Putative Pathogenic Gene Variants in UK Biobank Participants. *Circulation.* 2022;146(2):110–24.

16. Massier M, de Groote P, Donal E, Magnin-Poull I, Coubes C, Le Guillou Horn X, et al. Exploring the Familial Phenotypic Variability Associated With TTN Truncating Variants in Cardiomyopathies: Variant Spectrum, Genotype-Phenotype Correlation and Consequences in Genetic Counseling. *Clin Genet.* 2025;107(4):425–33.

17. Deep 6 AI. Artificial intelligence in clinical research [Internet]. Deep 6 AI. Pasadena, CA: Deep 6 AI; 2024. Available from: https://www.deep6.ai/. Accessed October 16, 2025.

18. Kinnamon DD, Morales A, Bowen DJ, Burke W, Hershberger RE, and Consortium* DCM. Toward Genetics-Driven Early Intervention in Dilated Cardiomyopathy: Design and Implementation of the DCM Precision Medicine Study. *Circ Cardiovasc Genet.* 2017;10(6).

19. Vasan RS, Larson MG, Levy D, Evans JC, and Benjamin EJ. Distribution and categorization of echocardiographic measurements in relation to reference limits: the Framingham Heart Study: formulation of a height- and sex-specific classification and its prospective validation. *Circulation.* 1997;96(6):1863–73.

20. Wilcox JE, Fang JC, Margulies KB, and Mann DL. Heart Failure With Recovered Left Ventricular Ejection Fraction: JACC Scientific Expert Panel. *J Am Coll Cardiol.* 2020;76(6):719–34.

21. Cao L, Rushakoff J, Williamson I, Karlstaedt A, Kittleson M, Czer L, et al. Similar burden of rare genetic variants in ischemic and non-ischemic dilated cardiomyopathy. *Front Cardiovasc Med.* 2025;12:1542653.

22. Jordan E, Peterson L, Ai T, Asatryan B, Bronicki L, Brown E, et al. Evidence-Based Assessment of Genes in Dilated Cardiomyopathy. *Circulation.* 2021;144(1):7–19.

23. McLaren W, Gil L, Hunt SE, Riat HS, Ritchie GR, Thormann A, et al. The Ensembl Variant Effect Predictor. *Genome Biol.* 2016;17(1):122.

24. Mudge JM, Carbonell-Sala S, Diekhans M, Martinez JG, Hunt T, Jungreis I, et al. GENCODE 2025: reference gene annotation for human and mouse. *Nucleic Acids Res.* 2025;53(D1):D966–D75.

25. Wissel D, Mehlferber MM, Nguyen KM, Pavelko V, Tseng E, Robinson MD, et al. A Systematic Benchmark of High-Accuracy PacBio Long-Read RNA Sequencing for Transcript-Level Quantification. *bioRxiv.* 2025.

26. Zare Jousheghani Z, Singh NP, and Patro R. Oarfish: enhanced probabilistic modeling leads to improved accuracy in long read transcriptome quantification. *Bioinformatics.* 2025;41(Supplement_1):i304–i13.

27. Jin H, Wan YW, and Liu Z. Comprehensive evaluation of RNA-seq quantification methods for linearity. *BMC Bioinformatics.* 2017;18(Suppl 4):117.

28. Salim A, Bhuva DD, Chen C, Tan CW, Yang P, Davis MJ, et al. SpaNorm: spatially-aware normalization for spatial transcriptomics data. *Genome Biol.* 2025;26(1):109.

29. Moses L, Einarsson PH, Jackson K, Luebbert L, Booeshaghi AS, Antonsson S, et al. Voyager: exploratory single-cell genomics data analysis with geospatial statistics. *bioRxiv.* 2023.

30. Huber W, Carey VJ, Gentleman R, Anders S, Carlson M, Carvalho BS, et al. Orchestrating high-throughput genomic analysis with Bioconductor. *Nat Methods.* 2015;12(2):115–21.

31. Pages H, Aboyoun P, Gentleman R, DebRoy S. Biostrings: Efficient manipulation of biological strings (R package version 2.76.0) [Computer program]. Bioconductor. Available from: https://bioconductor.org/packages/Biostrings. Accessed October 16, 2025.

32. Wang ET, Sandberg R, Luo S, Khrebtukova I, Zhang L, Mayr C, et al. Alternative isoform regulation in human tissue transcriptomes. *Nature.* 2008;456(7221):470–6.

33. Meddeb M, Koleini N, Binek A, Keykhaei M, Darehgazani R, Kwon S, et al. Myocardial ultrastructure of human heart failure with preserved ejection fraction. *Nat Cardiovasc Res.* 2024;3(8):907–14.

34. Mc Ardle A, Binek A, Moradian A, Chazarin Orgel B, Rivas A, Washington KE, et al. Standardized Workflow for Precise Mid- and High-Throughput Proteomics of Blood Biofluids. *Clin Chem.* 2022;68(3):450–60.

35. Robinson AE, Binek A, Venkatraman V, Searle BC, Holewinski RJ, Rosenberger G, et al. Lysine and Arginine Protein Post-translational Modifications by Enhanced DIA Libraries: Quantification in Murine Liver Disease. *J Proteome Res.* 2020;19(10):4163–78.

36. Demichev V, Messner CB, Vernardis SI, Lilley KS, and Ralser M. DIA-NN: neural networks and interference correction enable deep proteome coverage in high throughput. *Nat Methods.* 2020;17(1):41–4.

37. Therneau TM, and Grambsch PM. *Modeling Survival Data: Extending the Cox Model.* Springer; 2014.

38. Wickham H. *ggplot2: Elegant Graphics for Data Analysis.* Springer International Publishing; 2016.

39. Chicco D, and Jurman G. The advantages of the Matthews correlation coefficient (MCC) over F1 score and accuracy in binary classification evaluation. *BMC Genomics.* 2020;21(1):6.

40. R Core Team. R: A language and environment for statistical computing (version 4.5.0) [Computer program]. R Foundation for Statistical Computing; 2025. Available from: https://www.R-project.org/.

41. Romano R, Ghahremani S, Zimmerman T, Legere N, Thakar K, Ladha FA, et al. Reading Frame Repair of TTN Truncation Variants Restores Titin Quantity and Functions. *Circulation.* 2022;145(3):194–205.

42. Min KH, Go AS, Lee K, Parikh RV, Horiuchi KM, Ambrosy AP, et al. Guideline-Directed Medical Therapy and Outcomes Among Patients With Heart Failure With Improved Ejection Fraction. *J Am Coll Cardiol.* 2025;86(5):338–50.

43. Kao DP, Lowes BD, Gilbert EM, Minobe W, Epperson LE, Meyer LK, et al. Therapeutic Molecular Phenotype of beta-Blocker-Associated Reverse-Remodeling in Nonischemic Dilated Cardiomyopathy. *Circ Cardiovasc Genet.* 2015;8(2):270–83.

44. Xie M, Burchfield JS, and Hill JA. Pathological ventricular remodeling: therapies: part 2 of 2. *Circulation.* 2013;128(9):1021–30.

45. Deo RC. Alternative Splicing, Internal Promoter, Nonsense-Mediated Decay, or All Three: Explaining the Distribution of Truncation Variants in Titin. *Circ Cardiovasc Genet.* 2016;9(5):419–25.

46. Zaunbrecher RJ, Abel AN, Beussman K, Leonard A, von Frieling-Salewsky M, Fields PA, et al. Cronos Titin Is Expressed in Human Cardiomyocytes and Necessary for Normal Sarcomere Function. *Circulation.* 2019;140(20):1647–60.

47. Kellermayer D, Tordai H, Kiss B, Torok G, Peter DM, Sayour AA, et al. Truncated titin is structurally integrated into the human dilated cardiomyopathic sarcomere. *J Clin Invest.* 2024;134(2).

48. McAfee Q, Caporizzo MA, Uchida K, Bedi KC, Jr., Margulies KB, Arany Z, et al. Truncated titin protein in dilated cardiomyopathy incorporates into the sarcomere and transmits force. *J Clin Invest.* 2024;134(2).

Figure 1

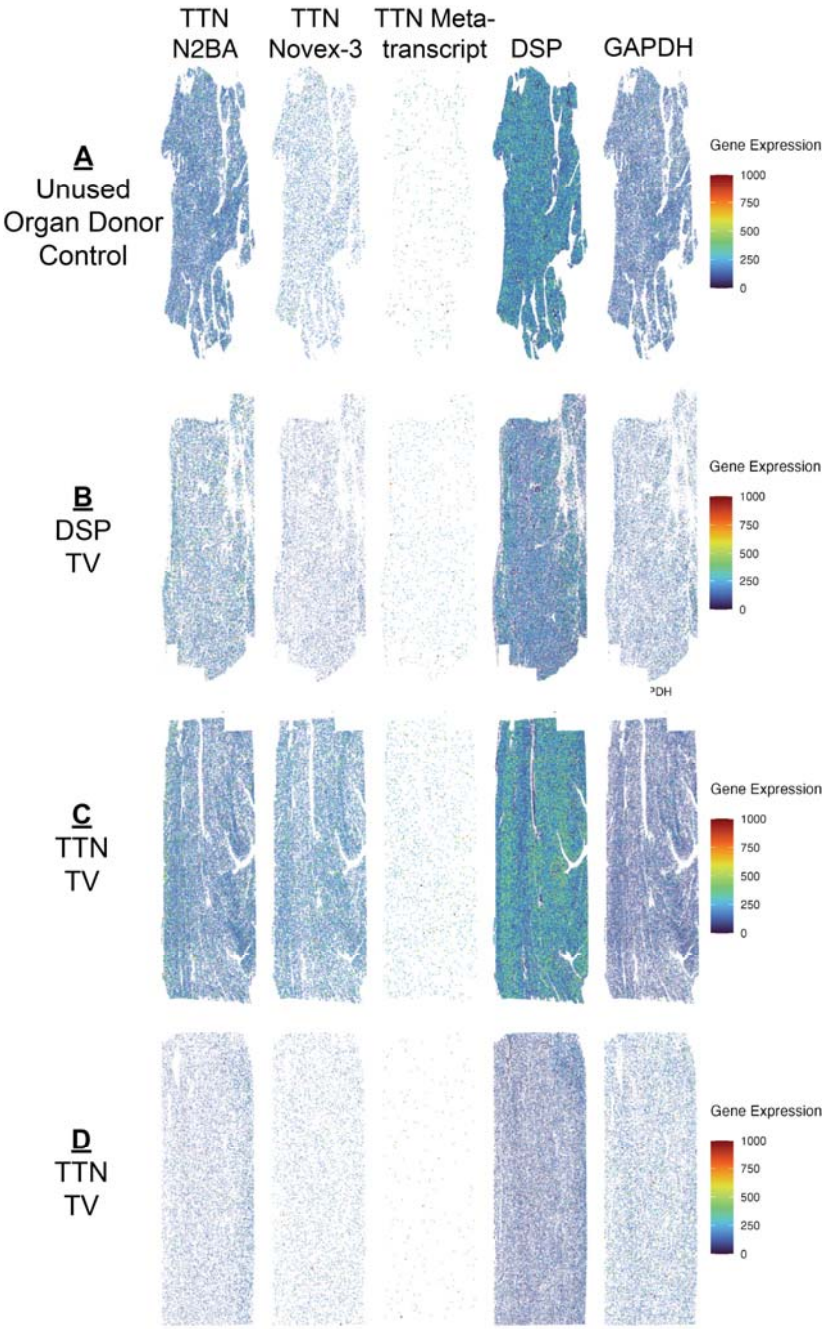

Figure 1: Spatial transcriptomics using explanted heart tissue obtained from (A) unused organ donor, (B) patient with DCM due to a *DSP* truncating variant, and (C and D) two patients with DCM due to TTN-TV. Using probes specific for the N2BA, Novex-3, and meta-transcript TTN isoforms, we found that the ratio of Novex-3:N2BA and meta-transcript:N2BA was similar between all four donors and yielded similar values to those measured using long-read RNA sequencing.

Figure 2

A

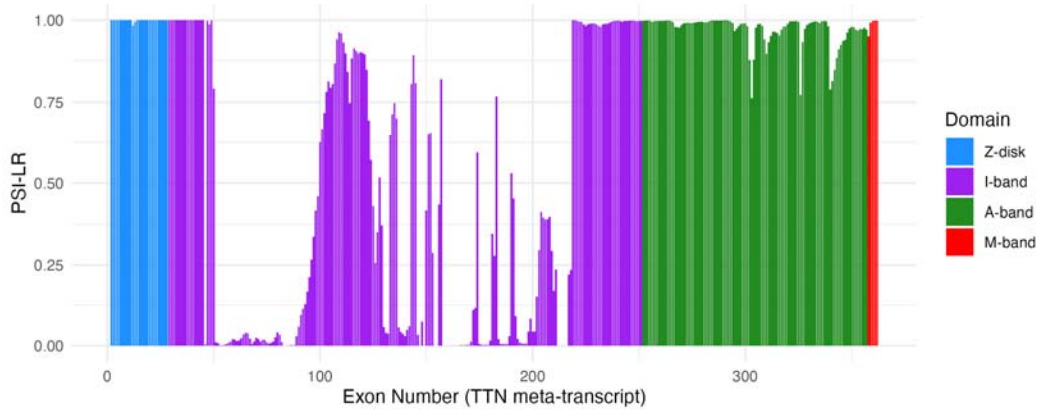

B

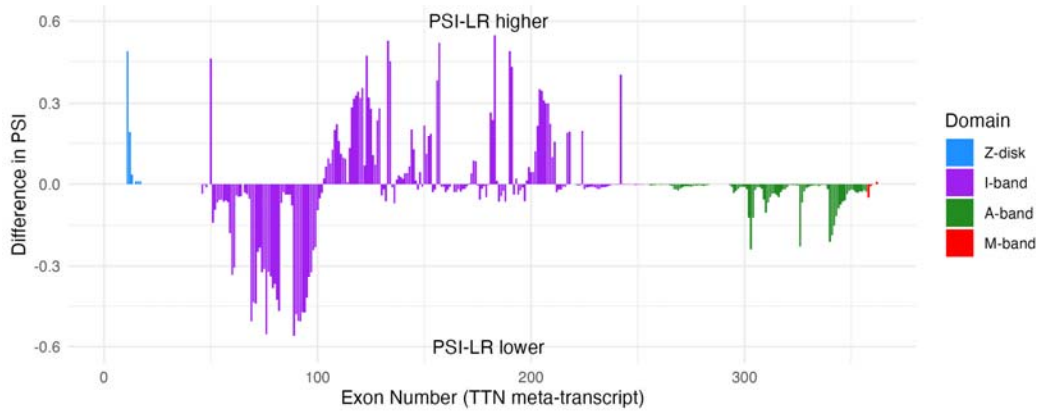

C

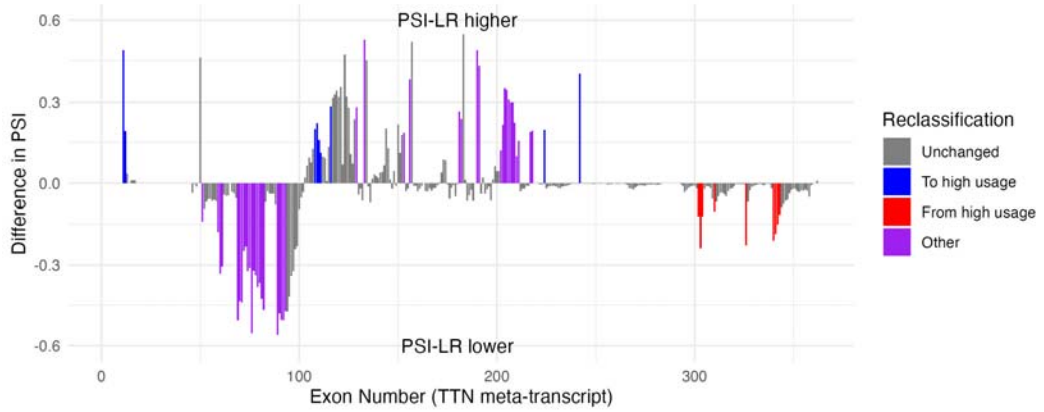

Figure 2: Comparison of percent spliced in (PSI)-long-read (PSI-LR) and PSI-short-read (PSI-SR) values. (A) Plot of PSI-LR values against exon number in the TTN meta-transcript. (B) Difference in value between PSI-LR and PSI-SR by exon number in the TTN meta-transcript. Positive values indicate that PSI-LR > PSI-SR. (C) Reclassification of exon usage by using PSI-LR as compared to PSI-SR. Exons in blue moved to the high usage group (PSI > 0.9) and exons in red moved from the high usage group to the low (PSI < 0.15) or intermediate (PSI 0.15 - 0.9) usage groups.

Figure 3

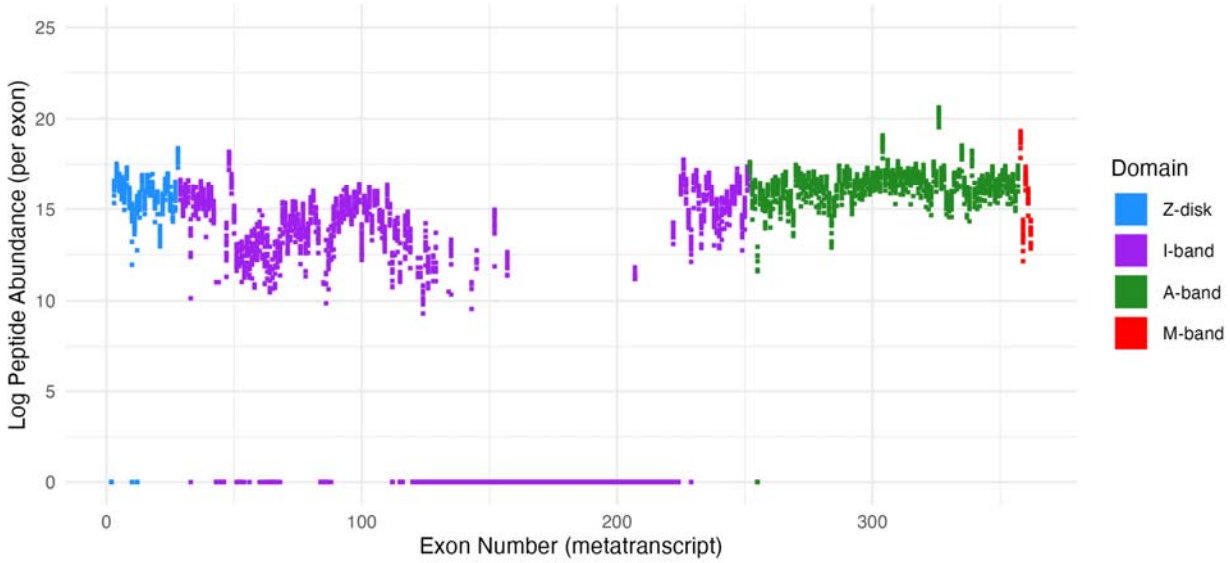

Figure 3: Peptide abundance for each domain of TTN determined using mass spectrometry-based proteomics. Log peptide abundance for each of the 14 DCM samples is plotted against exon number.

Figure 4

A

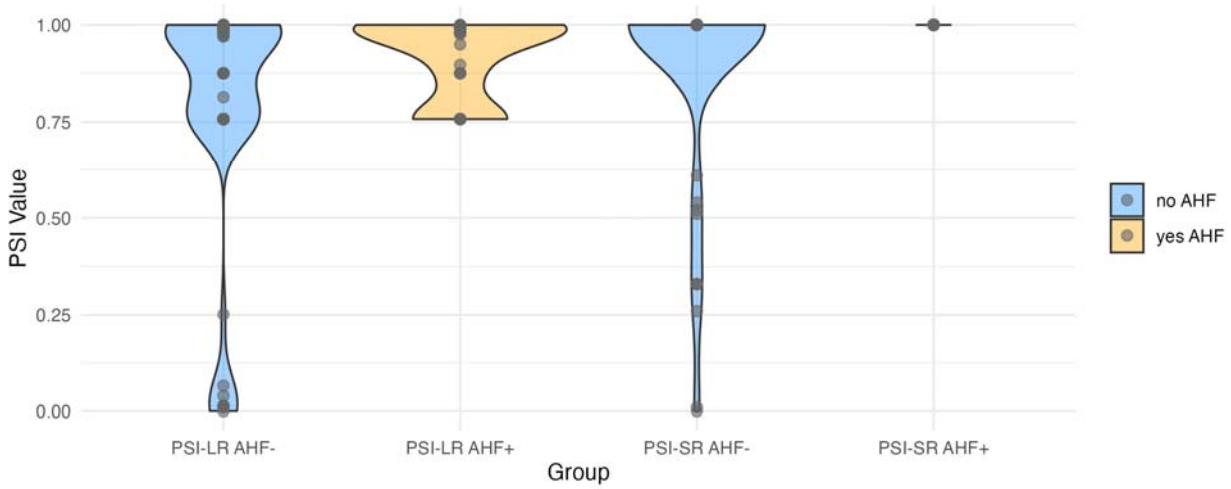

B

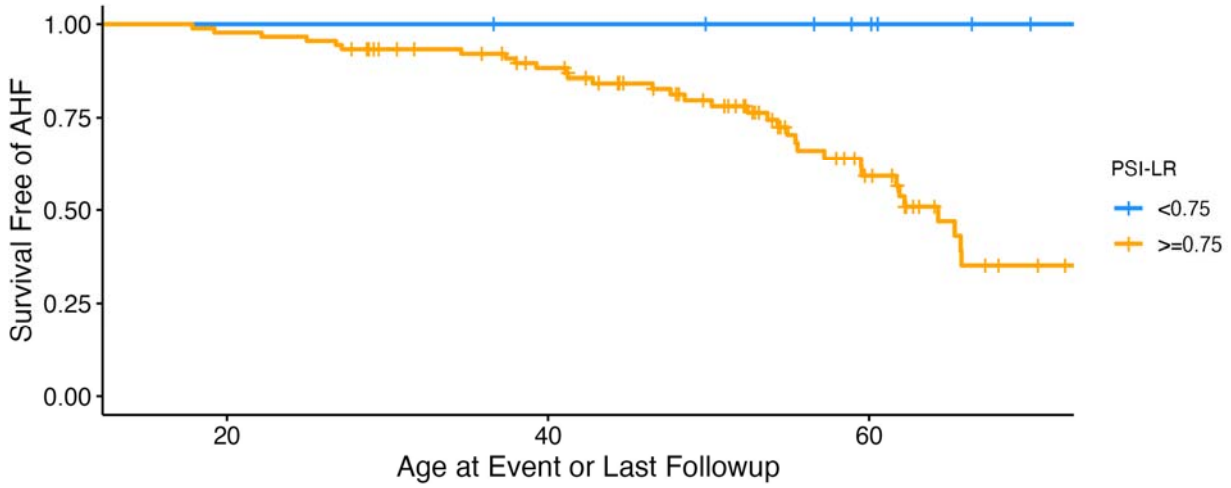

Figure 4: Relationship between percent spliced in (PSI) values and outcomes in the cardiomyopathy due to a TTN truncating variant (CM-TTN-TV) group. (A) PSI-LR values were lower in patients that developed AHF (median 0.98, range 0.76-1.00) as compared to PSI-SR values in the same patients (all 1.00, $p<0.001$). (B) Kaplan-Meier plot of survival free of AHF in CM-TTN-TV patients with PSI-LR < 0.75 (blue) or PSI-LR ≥ 0.75. No patients in the group with PSI-LR < 0.75 developed AHF during follow up.

Table 1: Comparison of *TTN* transcript isoform expression among unused donor hearts (control), dilated cardiomyopathy not due to a TTN truncating variant, and dilated cardiomyopathy due to a TTN truncating variant.

Transcript	Control n=8	Non-TTN-TV DCM N=7	TTN-TV DCM N=7	P-value
N2BA	223 [212;261]	90.7 [57.0;204]	149 [126;171]	0.031
Novex3	76.6 [67.4;84.5]	33.1 [22.5;52.0]	54.1 [42.5;67.7]	0.003
N2B	37.0 [32.0;39.8]	16.2 [14.5;34.1]	46.6 [34.7;59.4]	0.183
TTN-208	27.0 [21.1;33.5]	6.37 [3.54;10.5]	11.3 [10.1;19.3]	0.002
TTN-211	34.2 [29.7;39.8]	1.32 [1.19;2.16]	4.46 [3.19;10.6]	<0.001
TTN-206	6.61 [3.61;12.9]	5.13 [4.33;13.3]	9.51 [8.17;12.7]	0.740
TTN-215	11.7 [9.61;19.0]	2.88 [2.61;5.77]	5.95 [4.52;6.82]	0.004
N2A	7.95 [6.95;9.99]	3.10 [2.17;8.55]	3.09 [2.24;5.03]	0.031
Meta	1.66 [0.85;4.27]	3.10 [2.65;5.59]	5.72 [4.11;9.41]	0.102
TTN-207	2.39 [1.84;2.96]	0.90 [0.53;4.16]	2.80 [1.61;2.96]	0.925
TTN-214	2.80 [2.16;2.93]	1.20 [0.88;2.22]	2.25 [2.05;2.38]	0.057
TTN-205	0.97 [0.91;1.45]	1.14 [0.84;1.80]	0.65 [0.51;1.19]	0.496
TTN-209	0.69 [0.18;0.82]	0.57 [0.26;1.32]	1.82 [0.88;2.19]	0.097
Novex2	0.49 [0.31;0.64]	0.12 [0.07;0.29]	0.23 [0.20;0.25]	0.107
Cronos	0.05 [0.04;0.10]	0.06 [0.05;0.15]	0.07 [0.06;0.17]	0.701

Note: Expression levels are provided in transcripts per million.

Abbreviations: DCM = dilated cardiomyopathy; TTN-TV = titin truncating variant. Data presented as median [1st quartile; 3rd quartile]. P-value is from Kruskall-Wallis test.

Table 2: General characteristics and echocardiographic parameters of dilated cardiomyopathy patients with TTN truncating variants based on whether they developed advance heart failure.

Characteristics	DCM Patients Without AHF n=64	DCM Patients With AHF n=34	P-value
Characteristics			
Age of onset	50.1 [37.1;58.5]	43.5 [36.5;51.6]	0.095
Sex			0.066
Women	22 (34.4%)	5 (14.7%)	
Men	42 (65.6%)	29 (85.3%)	
Race			0.070
Asian	6 (9.38%)	2 (5.88%)	
Black	4 (6.25%)	8 (23.5%)	
Other	5 (7.81%)	4 (11.8%)	
White	49 (76.6%)	20 (58.8%)	
Ethnicity: Hispanic	5 (7.8%)	3 (8.8%)	1.000
Diabetes mellitus	11 (17.2%)	11 (32.4%)	0.145
Hypertension	20 (31.2%)	19 (55.9%)	0.031
Systolic BP	116 [107;129]	106 [96.5;116]	0.005
History of AF	27 (45.0%)	20 (60.6%)	0.221
History of VT	20 (33.3%)	25 (75.8%)	<0.001
Echocardiographic Parameters			
EF: First	27.5 [19.5;41.2]	20.0 [15.0;27.5]	0.016
LVEDD: First	58.0 (8.09)	64.9 (12.7)	0.020
LVD: First	40 (66.7%)	23 (88.5%)	0.067
EF: Last	43.5 [36.5;52.0]	15.5 [15.0;20.0]	<0.001
LVEDD:	54.0 [50.0;58.5]	67.0 [60.0;72.5]	<0.001
Change in EF	12.7 (15.0)	-4.5 (10.0)	<0.001
LVRR	33 (51.6%)	1 (2.9%)	<0.001

Abbreviations: AF = atrial fibrillation; AHF = advanced heart failure; BP = blood pressure; DCM = dilated cardiomyopathy; LV = left ventricular dilation; LVEDD = left ventricular end-diastolic diameter; LVRR = left ventricular reverse remodeling; VT = ventricular tachycardia.

Table 3: Genetic characteristics of dilated cardiomyopathy patients with TTN truncating variants based on whether they developed advance heart failure.

Characteristics	DCM Patients Without AHF n=64	DCM Patients With AHF n=34	P-value
Consequence			0.267
stop codon	27 (42.2%)	14 (41.2%)	
frameshift	29 (45.3%)	19 (55.9%)	
canonical splice	8 (12.5%)	1 (2.94%)	
Domain			0.159
Z-disk	3 (4.76%)	1 (2.94%)	
I-band	15 (23.8%)	3 (8.82%)	
A-band	45 (71.4%)	30 (88.2%)	
Exon number	304 [229; 326]	316 [273; 326]	0.199
Exon utilization: PSI-LR			0.071
0.00-0.14	8 (12.5%)	0 (0.00%)	
0.15-0.90	26 (40.6%)	13 (38.2%)	
0.91-1.00	30 (46.9%)	21 (61.8%)	
Exon utilization: PSI-SR			0.042
0.00-0.14	2 (3.12%)	0 (0.00%)	
0.15-0.90	8 (12.5%)	0 (0.00%)	
0.91-1.00	54 (84.4%)	34 (100%)	

Abbreviations: AF = atrial fibrillation; AHF = advanced heart failure; BP = blood pressure; DCM = dilated cardiomyopathy; LVEDD = left ventricular end-diastolic diameter; PSI-LR = percent spliced in long-read; PSI-SR = percent spliced in short-read; VT = ventricular tachycardia.

Table 4: Results of univariate logistic model for advanced heart failure with general and genetic characteristics as potential predictors.

Variable	Odds Ratio	95% Confidence Interval	p-value
Age of onset	0.78	0.57-1.06	0.113
Sex: women	0.33	0.11-0.97	0.044
Race			
Asian/Other	1.47	0.47-4.59	0.507
Black	4.90	1.33-18.1	0.017
White	Reference	Reference	Reference
Diabetes mellitus	2.30	0.88-6.1	0.091
Hypertension	2.79	1.18-6.58	0.019
Domain			
A-band	Reference	Reference	Reference
I/Z-band	0.33	0.10-1.08	0.068
Exon utilization			
PSI-LR	1.35	1.02-1.79	0.038
PSI-SR	47.8	0-Inf	0.991
Peptide abundance	1.03	0.91-1.16	0.680

Notes: Age is per decade; exon length is per 1000 nucleotides; PSI is per 0.1 increase.

Abbreviations: DCM = dilated cardiomyopathy; PSI-LR = percent spliced in long-read; PSI-SR = percent spliced in short-read.